GEOLOGICA CARPATHICA, 53, 1, BRATISLAVA, FEBRUARY 2002
45–52

$^{40}Ar/^{39}Ar$ DATING OF ALKALINE LAMPROPHYRES FROM THE POLISH WESTERN CARPATHIANS

ANNA LUCIŃSKA-ANCZKIEWICZ[1†], IGOR M. VILLA[2], ROBERT ANCZKIEWICZ[3*] and ANDRZEJ ŚLĄCZKA[1]

[1]Geological Institute, Jagiellonian University, ul. Oleandry 2a, Kraków, Poland
[2]Laboratorium für Isotopengeologie, Mineralogisch-Petrografisches Institut, Universität Bern, Erlachstrasse 9a, CH-3012 Bern, Switzerland
[3]Institute of Geological Sciences, Polish Academy of Sciences, Kraków Research Centre, ul. Senacka 1, 31-002 Kraków, Poland

*Present address: Department of Geological Sciences, University College London, Gower Street, London WC1E 6BT, England
Robert Anczkiewicz, Department of Geological Sciences, University College London, Gower Street, London WC1E 6BT, England. Tel: +44 (0)20-7679-2260. Fax: +44 (0)20-7387-1612. E-mail: rob@gl.rhul.ac.uk

(Manuscript received April 18, 2001; accepted in revised form October 4, 2001)

Abstract: Amphiboles from two types of alkaline lamprophyres from the Silesian Nappe in the Polish Western Carpathians were dated by $^{40}Ar/^{39}Ar$ stepwise heating technique. Three teschenite samples representing mesocratic type of lamprophyres yielded similar ages of 122.3±1.6 Ma, while leucocratic lamprophyre represented by a syenite dyke gave 120.4±1.4 Ma date. These ages are interpreted as the time of magmatic emplacement during Early Cretaceous extensional episode within the Silesian Basin. Ages for both types of lamprophyres are identical within error limits, which points to fast (probably ca. 5 Ma) magma evolution from meso to leucocratic stage.

Keywords: Early Cretaceous, Western Carpathians, teschenites, lamprophyres, $^{40}Ar/^{39}Ar$ geochronology.

Introduction

Lamprophyres in the Western Carpathians, usually known as teschenites or Teschenite Association Rocks (TAR), spread out from Nový Jičín (NE Moravia) in Czech Republic to Bielsko-Biała in S-Poland (Fig. 1). They represent hypabyssal intrusions and extrusions of alkaline magma. Although most of the researchers agree on their Early Cretaceous age (Kudlásková 1987; Suk 1984; Šmíd 1962; Hovorka & Spišiak 1988), the precise timing of this magmatic event remains unknown. For instance, in the Polish Carpathians TAR are most abundant in the Tithonian-Neocomian beds, which lead Smulikowski (1980) to propose that magmatic activity lasted from Tithonian to the end of Neocomian. On the other hand Nowak (1978) linked TAR to the Barremian–Aptian magmatic cycle.

In order to provide tighter constraints on the timing of this important magmatic episode, we dated four TAR samples using $^{40}Ar/^{39}Ar$ technique. Two dominant petrological types of TAR from the Polish Western Carpathians representing different stages of magma evolution were subjected to geochronological and petrological studies.

Geological setting

The Outer Western Carpathians (Fig. 1) consist of several nappes composed dominantly of flysch deposits and minor volcanites, volcaniclastites and igneous intrusions. From N to S the main units are: the Skole, Subsilesian, Silesian, Dukla-Foremagura and Magura Nappes (Figs. 1 and 2) (Książkiewicz 1972). They are commonly correlated with Alpine flysch deposits and hence reflect Mesozoic-Paleogene sedimentation in distinct basins on the Tethys northern margin (Csontos et al. 1992). Their present tectonic juxtaposition is due to Neogene northward thrusting and nappe formation. The occurrence of TAR is limited to the Silesian Nappe, whose ca. 7 km thick sedimentary sequence represents the time span from late Kimmeridgian to Early Miocene. In the Polish part of the Silesian Nappe TAR occur in the Cieszyn Limestones (Upper Tithonian–Berriasian) and in the Upper Cieszyn Beds (Valanginian–Hauterivian) (Burtanówna et al. 1937).

TAR form hypabyssal intrusions, usually sills, rarely dykes with the exception of the Moravian part of the Silesian Nappe, where they occur as volcanic flows. Intrusions are most commonly tens of cm, exceptionally, tens of meters thick and usually show chilled margins. Host flysch deposits, at the contact with the intrusions, typically display narrow metamorphosed zones, which reached pyroxene hornfels facies (Wieser 1971).

Samples description

TAR outcrops in the Polish Western Carpathians are scarce. However, they form a wide variety of petrological types with various structures and textures (e.g. Hohenegger 1861; Tschermak 1866; Mahmood 1973; Smulikowski 1980; Kudlásková 1987; Dostal & Owen 1998). Commonly they are heterogeneous both on outcrop and even hand specimen scale. Additional difficulty in studying these rocks is caused by their poor preservation due to common secondary alterations linked to weathering and activity of hydrothermal fluids. After having investigated most of the known TAR exposures in the area, we selected four samples with the best preserved mineral assemblages from three localities within the Upper Cieszyn Beds. The selected rocks represent two petrological types reflecting different stages of magma differentiation: 1) Samples C-103,

† This paper is based on the early version of the manuscript by Anna Lucińska-Anczkiewicz, which was completed by co-authors. Ania died of cancer on 29 September 2000.

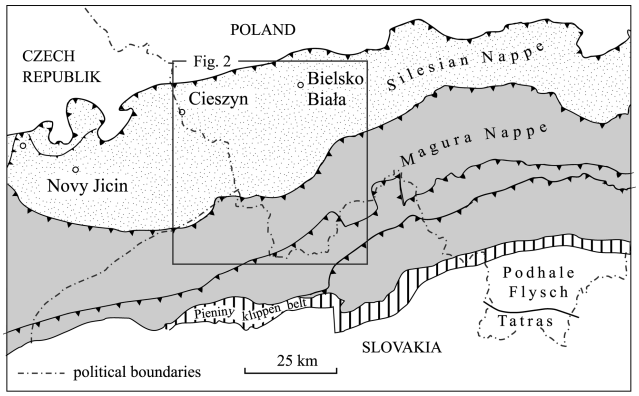

Fig. 1. Geological sketch of the Western Carpathians.

C-106 and C-200, termed as teschenites, are mesocratic and represent the most common type in the Polish Western Carpathians, 2) Sample C-53 represents leucocratic, more evolved magma, and was classified as syenite. Sample localities are marked in Fig. 2 and described below.

Sample C-103 is located in Boguszowice near Cieszyn next to the bridge on Olza river at the border between the Czech Republic and Poland (Fig. 2). The main rock forming assemblage is formed by (in order of decreasing abundance), pyroxene, brown amphibole, K-feldspar, analcime and apatite. Accessories are sphene, ilmenite, biotite and chlorite. Pyroxene and amphiboles form coarse, up to 2 cm long euhedral crystals. Seldom, amphiboles occur as elongated prismatic crystals. Both are commonly fractured and have tiny alteration rims. Amphiboles often contain inclusions of acicular apatite (very common) and rarer K-feldspar as well as analcime (Fig. 3a). Apatite crystals are up to 1 cm long. Sphene is the most common accessory phase and occurs as small (10–50 μm) euhedral crystals. Sporadic biotite (locally chloritized) and chlorite are up to 50 μm in size.

Analcime is usually a product of K-feldspar alteration, however, some of it can be primary. Precise relationship is difficult to asses due to very strong alterations. Also due to the breakdown of feldspathic minerals the rock has a secondary porphyritic texture with mafic minerals occurring as phenocrysts. This feature is typical for all three mesocratic teschenite samples.

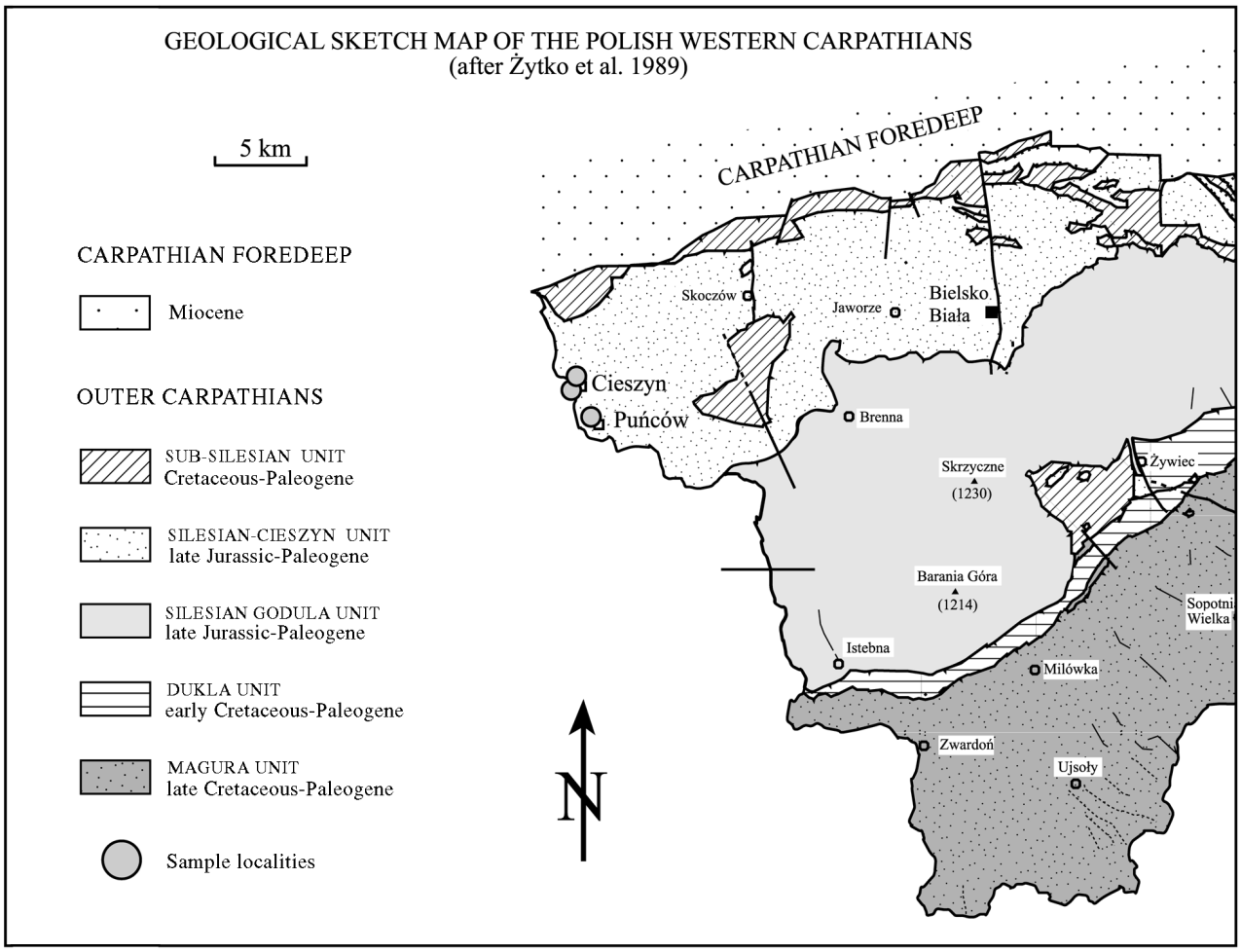

Fig. 2. Sample localities.

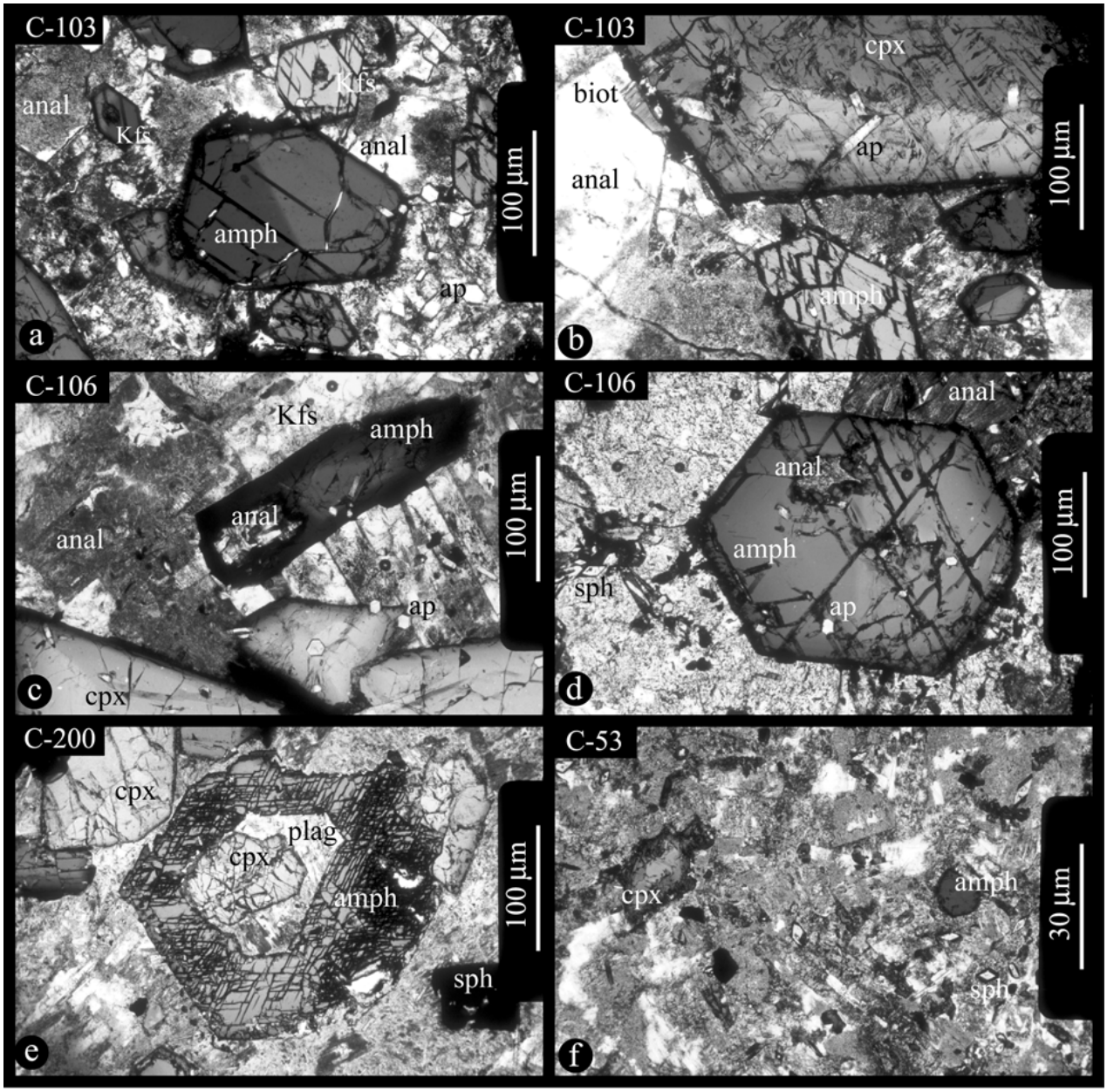

Fig. 3. Photomicrographs of the dated TAR: teschenites (**a**–**e**) and syenite (**f**). Amphibole and clinopyroxene crystals in altered matrix composed dominantly of secondary analcime and relict feldspar (a–e). All crystals show pronounced alterations on the rims. Most common inclusions within amphibole are K-feldspar (a), analcime (c) and apatite (d). Rare inclusions of clinopyroxene and plagioclase were observed in sample C-200 (e). Sample C-53 (syenite) (f) is fine-grained and contains crystals of clinopyroxene as and amphibole in altered matrix of feldspathic minerals. *Abbreviations:* Kfs — K-feldspar, anal — analcime, biot — biotite, amph — amphibole, cpx — clinopyroxene, sph — sphene, ap — apatite.

Sample C-106 was collected in the same locality as C-103. It is composed of pyroxene, brown amphibole, K-feldspar, analcime (mainly secondary, but see above) and apatite (Fig. 3c,d). Sphene, ilmenite and magnetite occur as accessory minerals. Pyroxene and amphibole form coarse euhedral or rarer sub-hedral crystals. Their size varies from ca. 0.5 cm at average up to 2 cm (Fig. 3c,d). Amphibole is usually present as coarse and seldom as acicular crystals. Similarly to the previous sample, the edges of amphiboles and pyroxenes commonly show certain degree of secondary alterations. Inclusions in amphibole are rather common. They consist mainly of apatite, rarer K-feldspar and analcime (Fig. 3c,d).

C-200 was collected in Rudów, north of Cieszyn in the Piotrówka stream bed (Fig. 2). The main minerals are: brown amphibole, pyroxene, analcime, K-feldspar with accessory biotite, chlorite, and sphene. In comparison with the two samples described above this sample contains a considerably smaller amount of apatite. Amphiboles and pyroxenes are less fractured. Similarly to previous samples inclusions in amphib-

oles are common and consist of K-feldspar, analcime and subordinate apatite (Fig. 3e). In this sample we observed pyroxene inclusions in amphibole, which are likely to be present also in other samples (Fig. 3e).

C-53 classified as syenite is located south of Cieszyn, ca. 1.5 km north of the church in Puńców village. The sample was collected from a small (ca. 15–20 cm wide) dyke, which intrudes teschenites, similar to the type described above. The rock is fine-grained, composed of green and brown pyroxenes, brown amphibole, K-feldspar, plagioclase, analcime (secondary), sphene, calcite, biotite and chlorite (Fig. 3f). Biotite is usually chloritized.

Amphibole is much less abundant in this sample. It occurs dominantly as acicular crystals, is poorer in inclusions (among investigated thin sections we only rarely observed analcime) but also shows pronounced marginal alterations. Similarly to amphibole, other minerals suffered strong secondary alterations.

Chemistry of amphiboles and their inclusions

Because of potential influence of K-bearing "contaminants" on K-Ar isotopic systematics, chemical composition of amphiboles as well as their alteration products and inclusions are of major importance for interpreting dating results. Ca and K are of particular interest because they are directly measured during mass spectrometric analyses and can be directly compared with the microprobe results. Such observations help to evaluate contribution of inclusions to the K-Ar budget in amphibole separates. Quantitative electron microprobe analyses of amphiboles and their inclusions are summarized in Table 1.

Amphibole crystals usually stay within kaersutite composition (classification after Leake et al. 1997), however, they show pronounced major elements zonation (Table 1). From core to rim there is a significant increase in the Fe content, which is compensated mainly by the decrease in Mg as well as by a smaller drop in Ca and Na. Ti content is rather constant throughout the grains. Sometimes a small decrease towards the rim was detected, however, usually it was not larger than 0.5 wt. % of TiO_2 (commonly much less). Between core and rim, there is usually a small increase of Ti. The K_2O content ranges from ca. 1.5–2.0 wt. % and stays rather constant within individual grains. Similar zonation of amphiboles was observed by Kudlásková (1987) and Dostal & Owen (1998).

Commonly kaersutite has tiny alteration rims, which relatively to core are enriched in Fe (> 20 wt. % FeO), K and slightly in Mn but depleted in Ti, Ca, Mg and Na (Table 1). Those alteration rims show a significant increase in the K_2O content, which can reach even 6 wt. %.

Average Ca/K ratio in kaersutite obtained by microprobe measurements is close to 7 but the ratios range between ca. 5.2 and 7.5. The strongest affect on K have alkali feldspars, whose K_2O content is even up to 10 times higher than this of kaersutite (Table 1). Additional contribution to K-Ar budget is from analcime, whose K content is comparable with that of amphibole. Similarly Ca is affected by cpx inclusions, however, they seem to be rare (Table 1). Certain amount of cpx is likely to be present also as "impurity" in amphibole concentrate, which was unavoidable during sample separation.

Because of different retentivity of K-Ar system by amphiboles and their inclusions and theirs different resistance to secondary alteration, complexities in $^{40}Ar/^{39}Ar$ age spectra were expected (see below).

$^{40}Ar/^{39}Ar$ dating results

Amphibole separates were prepared according to standard mineral separation procedures i.e. crushing and sieving followed by heavy liquid and magnetic separation. The final separates were "purified" by handpicking under stereomicroscope.

$^{40}Ar/^{39}Ar$ analyses and data presentation follow Belluso et al. (2000) and Villa et al. (2000). A summary of the isotopic results is presented in Table 2 and Figs. 4–8. All errors are given at the 1σ level.

Age spectra of samples representing mesocratic teschenite (C-103, C-106, C-200) generally show slowly rising apparent ages (except for sample C-103) with increasing degassing temperature for the first 15 % of ^{39}Ar released (Figs. 4–6). Apparent ages vary from 62 to 125 Ma with exception of sample C-103, which shows 162.5 Ma age for the first step (Fig. 4). This is most likely due to small amount of excess Ar component. Then the spectra stabilize at ca. 120–122 Ma until ca. 70 % of gas released. The final steps are again scattered, however, to a much lesser extent when compared with the low temperature steps.

All three teschenite age spectra show good correlation with the Ca/K ratios. Scatter observed within the low temperature apparent ages correlates with low, steadily increasing Ca/K ratios (Figs. 4–6). This is probably due to disturbance in the K-Ar system related to secondary alterations (see sample description) and contribution to K-Ar budget from inclusions like K-feldspar, which is altered itself and is likely to outgas at low temperature. These lower temperature steps are followed by the most stable middle part of the spectrum, which have Ca/K ratios between 6.3 and 7.5. The gas rich steps (10 % of the total Ar release or more) of the mesocratic samples (C-103, C-106 and C-200) have surprisingly constant Ca/K ratios of 7.5. These values are very close or the same as those obtained by the microprobe analyses for pure kaersutite (Table 1, Figs. 4–6). The best correlation was obtained for sample C-200, for which Ca/K ratios obtained by both techniques are the same. For other two samples the values obtained during mass spectrometric analyses are only slightly lower. During the high temperature gas release, small disturbances become visible; the disturbed steps correspond to higher Ca/K ratios (10.8 for C-103 and 15 for C-106) (Figs. 4, 5 and Table 2). We also note that the average age of the Ca-rich steps in C-106 and C-103 are identical to the age of the steps with Ca/K= 7.5. We interpret this as a reflection of a zonation of amphiboles, in which a more calcic kaersutite also gives step ages, which on average are identical to the most gas rich steps. We propose that pyroxene inclusions did not contribute significantly to the Ar budget, as pyroxene have Ca/K ratios exceeding 100.

For the final age calculations we used only steps whose Ca/K ratio is constant (therefore we will term the age so calculat-

Table 1: Representative microprobe analyses of amphiboles, their inclusions and pyroxens.

	Sample C-103						Sample C-106					Sample C-200			Sample C-53							
	Amph core	Amph rim	Kfs incl	Anal incl	Cpx core	Cpx rim	Amph core	Amph rim 1	Rim 2*	Cpx core	Cpx rim	Amph core	Amph rim	Cpx incl	Amph core	Amph rim	Anal incl	Kfs	Cpx brown core	Cpx brown rim	Cpx green core	Cpx green rim
SiO_2	37.34	37.03	63.64	53.82	40.73	43.55	37.61	35.65	31.45	43.34	41.41	37.03	37.03	45.98	35.68	34.73	53.79	65.89	44.03	39.73	42.49	46.45
TiO_2	6.16	5.76	0.02	0.02	5.64	3.88	5.89	5.59	1.37	4.12	4.79	6.67	5.76	2.63	4.67	4.69	0.02	0.02	2.21	3.72	2.63	0.95
Al_2O_3	14.90	15.05	18.35	26.25	11.79	10.00	13.76	14.88	13.19	9.18	10.93	12.77	14.55	8.04	13.81	13.69	23.46	17.79	5.75	8.74	6.19	2.48
FeO	13.05	14.82	0.33	0.00	9.78	10.32	10.32	18.60	37.12	8.22	10.39	12.69	14.81	8.98	19.94	21.35	0.01	0.28	13.01	17.32	21.99	23.19
MnO	0.22	0.25	0.03	0.76	0.14	0.22	0.09	0.37	1.14	0.13	0.22	0.00	0.21	0.15	0.39	0.42	0.02	0.00	0.36	0.59	0.84	1.13
MgO	10.10	8.97	0.00	0.00	8.62	8.43	11.86	6.20	1.93	10.47	8.23	11.52	8.67	9.33	6.18	5.17	0.00	0.00	8.00	4.28	2.42	2.85
CaO	12.59	12.48	0.16	0.12	24.19	23.82	12.85	12.09	0.11	24.21	23.81	14.32	13.48	25.04	12.59	12.36	0.01	0.20	24.65	23.87	22.92	21.81
Na_2O	2.58	2.15	0.77	11.20	0.80	0.83	2.14	2.28	0.08	0.57	0.66	1.73	1.95	0.10	2.45	2.28	13.00	4.57	0.62	0.78	1.03	1.54
K_2O	1.58	1.58	16.25	1.88	0.00	0.00	1.64	1.64	6.27	0.00	0.01	1.77	1.71	0.00	1.76	1.80	0.83	11.15	0.00	0.00	0.00	0.00
Total	98.52	98.09	99.55	94.05	101.69	101.05	96.16	97.30	92.66	100.24	100.45	98.50	98.17	100.25	97.47	96.49	91.14	99.90	98.63	99.03	100.51	100.40
Ca/K	6.82	6.76	0.01	0.05	----	----	6.70	6.31	0.02	----	1871	6.91	6.76	----	6.12	5.87	0.01	0.02	----	----	----	----
Oxygens in formula	23	23	8	6	6	6	23	23		6	6	23	23	6	23	23	6	8	6	6	6	6
Si	5.60	5.61	2.97	1.93	1.54	1.65	5.54	5.57		1.64	1.59	5.39	5.40	1.74	5.30	5.58	1.99	3.01	1.74	1.61	1.72	1.88
Ti	0.69	0.66	0.00	0.00	0.16	0.11	0.65	0.66		0.12	0.14	0.73	0.63	0.08	0.52	0.57	0.00	0.00	0.07	0.11	0.08	0.03
Al	2.63	2.69	1.01	1.11	0.53	0.45	2.39	2.74		0.41	0.49	2.19	2.50	0.36	2.42	2.59	1.02	0.96	0.27	0.42	0.30	0.12
Fe^{2+}	1.64	1.88	0.00	0.00	0.31	0.33	-0.04	2.43		0.26	0.33	-0.06	-0.08	0.25	-0.15	2.87	0.00	0.00	0.43	0.59	0.75	0.79
Mn	0.03	0.03	0.00	0.05	0.00	0.01	0.01	0.05		0.00	0.01	0.00	0.03	0.01	0.05	0.06	0.00	0.00	0.01	0.02	0.03	0.04
Mg	2.26	2.03	0.00	0.00	0.49	0.48	2.60	1.44		0.59	0.47	2.50	1.88	0.53	1.37	1.24	0.00	0.00	0.47	0.26	0.15	0.17
Ca	2.02	2.03	0.01	0.01	0.98	0.97	2.03	2.02		0.98	0.98	2.23	2.11	1.01	2.00	2.13	0.00	0.01	1.05	1.04	1.00	0.95
Na	0.75	0.63	0.07	0.78	0.06	0.06	0.61	0.69		0.04	0.05	0.49	0.55	0.01	0.71	0.71	0.93	0.40	0.05	0.06	0.08	0.12
K	0.30	0.31	0.97	0.09	0.00	0.00	0.31	0.33		0.00	0.00	0.33	0.32	0.00	0.33	0.37	0.04	0.65	0.00	0.00	0.00	0.00
Total	15.92	15.86	5.03	3.97	4.07	4.06	14.11	15.92		4.04	4.06	13.80	13.33	3.97	12.55	16.10	3.99	5.03	4.09	4.11	4.11	4.10

*Altered outermost rim of the same amphibole crystal. Total Fe as FeO. Abbreviations: Amph — amphibole, Kfs — K-feldspar, Anal — analcime, Cpx — clinopyroxene, incl — inclusion.

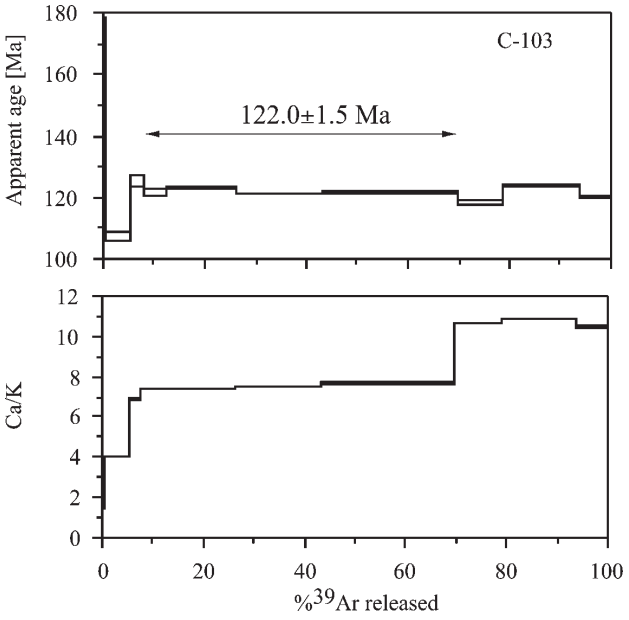

Fig. 4. $^{40}Ar/^{39}Ar$ results for sample C-103. (a) Age spectrum. (b) Ca/K vs. % ^{39}Ar released.

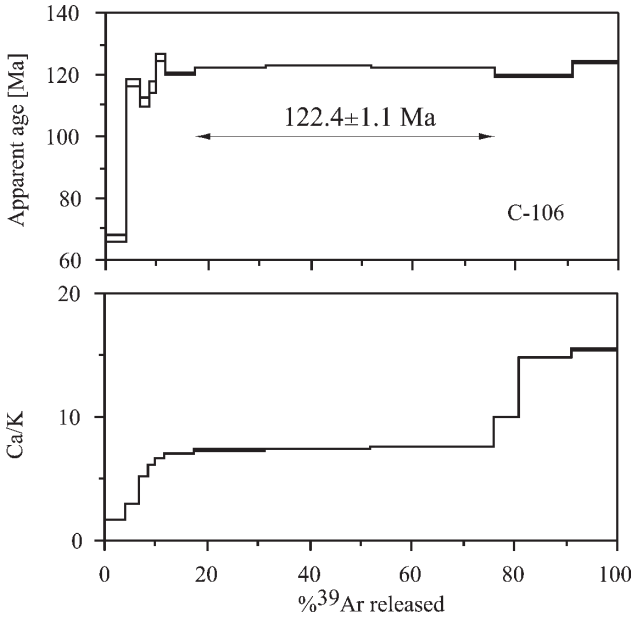

Fig. 5. $^{40}Ar/^{39}Ar$ results for sample C-106. (a) Age spectrum. (b) Ca/K vs. % ^{39}Ar released.

ed: "isochemical age") and close to the values obtained by microprobe analyses. The three mesocratic teschenite samples C-103, C-106 and C-200 yielded 122.0±1.5, 122.4±1.1, 122.2±0.9 Ma ages respectively (Figs. 4–6).

Syenite age spectrum (sample C-53) shows a low apparent age for the first 13 % ^{39}Ar released and then stabilizes at ca. 120 Ma until ca. 80 % of ^{39}Ar released (Fig. 7). Then the age spectrum forms a depression expressed by the drop of apparent ages down to 113 Ma, followed by the rise during the last two steps. This pattern again correlates with the Ca/K ratios (Fig. 7).

Low age for the first step is likely to be caused by some Ar loss due to secondary alteration, which is observed on the rims of the amphiboles in all investigated samples. A sudden drop in apparent ages followed by a subsequent rise is correlated with very high Ca/K ratios. This is interpreted as due to the presence of calcite in our mineral separate.

Table 2: Summary of $^{40}Ar/^{39}Ar$ dating results.

Step	Temp.	%^{39}Ar released	^{40}Ar tot. (pl/g)	1σ	^{40}Ar* (pl/g)	^{39}Ar (pl/g)	1σ	^{38}Ar (pl/g)	1σ	^{38}Ar(Cl) (pl/g)	^{37}Ar (pl/g)	1σ	^{36}Ar (pl/g)	1σ	Age	1σ
Sample C-103, weight = 0.022 g K = 0.70 wt.%, Ca = 5.3 wt.%, Cl = 169 ppm J = 0.006884																
1	400	0.30	5.66	0.01	3.19	0.23	0.00	0.019	0.002	0.015	0.18	0.01	0.008	0.001	162.5	16.0
2	956	4.86	68.79	0.00	33.54	3.78	0.00	0.419	0.002	0.353	7.62	0.03	0.121	0.002	107.1	1.5
3	975	2.62	23.42	0.01	21.28	2.04	0.00	0.258	0.002	0.234	7.00	0.03	0.009	0.001	125.5	1.8
4	996	4.67	39.66	0.01	36.75	3.63	0.00	0.427	0.002	0.385	13.39	0.04	0.013	0.001	121.8	1.0
5	1018	13.79	114.47	0.01	109.99	10.72	0.01	1.080	0.003	0.957	39.70	0.11	0.025	0.002	123.4	0.4
6	1033	17.04	138.32	0.01	133.50	13.25	0.01	1.270	0.003	1.118	49.44	0.14	0.029	0.001	121.3	0.2
7	1069	26.48	212.19	0.02	208.03	20.59	0.02	1.927	0.004	1.693	78.94	0.23	0.034	0.001	121.6	0.1
8	1070	9.03	77.99	0.01	68.95	7.02	0.01	1.109	0.003	1.026	37.31	0.10	0.040	0.001	118.4	0.6
9	1240	14.92	121.98	0.01	119.50	11.60	0.01	1.843	0.004	1.714	62.92	0.18	0.024	0.001	124.0	0.2
10	1408	6.28	52.82	0.00	48.66	4.88	0.01	0.734	0.002	0.677	25.51	0.07	0.021	0.001	120.2	0.7
															"Isochemical age" (steps 4–7) = 122.0±1.5 Ma	
Sample C-106, weight = 0.061 g K = 0.63 wt.%, Ca = 5.0 wt.%, Cl = 163 ppm J = 0.006884																
1	722	4.08	201.20	0.02	43.48	7.92	0.01	6.315	0.012	6.123	6.90	0.02	0.535	0.003	66.9	1.2
2	936	2.58	76.74	0.00	48.77	5.00	0.00	0.586	0.002	0.511	7.22	0.02	0.097	0.002	117.3	1.3
3	955	1.64	38.24	0.01	29.23	3.17	0.00	0.436	0.002	0.394	8.26	0.03	0.033	0.001	111.1	1.4
4	955	1.34	32.67	0.00	25.05	2.61	0.00	0.388	0.002	0.353	7.92	0.03	0.028	0.001	115.7	1.8
5	973	2.18	51.00	0.00	44.11	4.23	0.00	0.611	0.002	0.559	13.96	0.04	0.027	0.002	125.4	1.1
6	994	5.49	117.14	0.02	106.47	10.65	0.01	1.337	0.003	1.210	37.49	0.11	0.046	0.002	120.3	0.4
7	1014	13.88	286.86	0.03	273.57	26.93	0.02	2.613	0.005	2.302	98.33	0.27	0.070	0.001	122.3	0.2
8	1033	20.38	413.40	0.03	403.93	39.55	0.04	3.342	0.006	2.891	145.54	0.41	0.069	0.001	122.9	0.1
9	1072	24.29	486.92	0.02	477.91	47.14	0.04	3.818	0.007	3.284	178.86	0.49	0.076	0.002	122.0	0.1
10	1104	4.90	100.49	0.01	94.16	9.50	0.01	0.880	0.003	0.771	47.65	0.13	0.034	0.001	119.4	0.4
11	1241	10.23	207.44	0.02	196.53	19.85	0.02	1.991	0.004	1.772	146.52	0.40	0.074	0.002	119.5	0.2
12	1410	9.02	189.23	0.03	180.07	17.50	0.02	1.772	0.004	1.580	134.93	0.37	0.065	0.002	124.1	0.2
															"Isochemical age" (steps 7–9) = 122.4±1.1 Ma	
Sample C-200, weight = 0.087 g K = 0.70 wt.%, Ca = 4.9 wt.%, Cl = 127 ppm J= 0.006884																
1	724	1.44	145.83	0.02	22.48	4.46	0.01	0.280	0.002	0.150	5.26	0.02	0.419	0.002	61.6	1.6
2	936	2.72	100.43	0.00	81.84	8.39	0.01	1.161	0.003	1.053	16.54	0.05	0.067	0.002	117.4	0.6
3	957	2.31	78.15	0.01	70.88	7.13	0.01	1.273	0.003	1.187	20.64	0.06	0.030	0.002	119.6	0.7
4	973	2.02	76.97	0.01	62.46	6.25	0.01	0.981	0.003	0.901	20.70	0.06	0.054	0.001	120.3	0.6
5	995	4.38	149.83	0.01	136.02	13.53	0.01	1.584	0.004	1.423	49.13	0.13	0.059	0.002	121.0	0.4
6	1016	14.74	477.79	0.05	461.02	45.56	0.04	4.041	0.008	3.519	169.95	0.48	0.100	0.002	121.8	0.1
7	1031	22.33	715.79	0.06	704.09	69.00	0.06	5.556	0.010	4.773	257.91	0.72	0.105	0.002	122.8	0.1
8	1068	31.24	993.03	0.10	985.35	96.52	0.09	7.458	0.014	6.369	362.35	1.01	0.118	0.002	122.8	0.1
9	1104	6.19	199.97	0.02	194.49	19.11	0.02	1.831	0.004	1.613	77.17	0.22	0.038	0.002	122.5	0.2
10	1245	7.60	246.55	0.01	240.44	23.49	0.02	2.288	0.005	2.024	115.02	0.32	0.050	0.001	123.2	0.1
11	1412	5.04	170.22	0.02	161.19	15.57	0.01	1.605	0.003	1.427	73.75	0.21	0.049	0.002	124.6	0.3
															"Isochemical age" (steps 5–9) = 122.2±0.9 Ma	
Sample C-53, weight = 0.103 g K = 0.47 wt.%, Ca= 6.5 wt.%, Cl = 176 ppm J = 0.006884																
1	740	13.03	726.77	0.058	278.353	31.607	0.028	4.112	0.008	3.465	57.57	0.16	1.532	0.006	106.3	0.6
2	973	32.98	854.49	0.077	802.449	80.017	0.070	15.439	0.027	14.500	251.78	0.72	0.240	0.002	120.7	0.1
3	993	32.03	790.53	0.058	775.951	77.708	0.068	14.093	0.025	13.207	261.90	0.74	0.116	0.001	120.2	0.1
4	1009	3.48	87.10	0.007	81.762	8.453	0.008	1.461	0.003	1.363	33.24	0.09	0.027	0.002	116.6	0.5
5	1047	4.53	121.51	0.010	103.209	11.000	0.010	1.806	0.004	1.679	98.50	0.27	0.087	0.001	113.6	0.4
6	1058	4.05	106.01	0.008	90.580	9.814	0.009	1.661	0.004	1.569	232.94	0.63	0.112	0.002	112.9	0.4
7	1073	1.81	50.22	0.003	40.609	4.388	0.004	0.744	0.003	0.714	187.61	0.53	0.080	0.002	114.6	0.6
8	1109	1.78	55.68	0.009	39.884	4.321	0.005	0.778	0.003	0.755	259.39	0.75	0.120	0.001	115.6	0.7
9	1250	2.89	82.43	0.007	71.237	7.019	0.007	1.273	0.004	1.227	308.27	0.89	0.116	0.002	125.4	0.4
10	1413	3.41	95.39	0.007	86.479	8.272	0.007	1.522	0.003	1.442	162.78	0.45	0.072	0.001	127.0	0.3
															"Isochemical age" (steps 2–3) = 120.4±1.3 Ma	

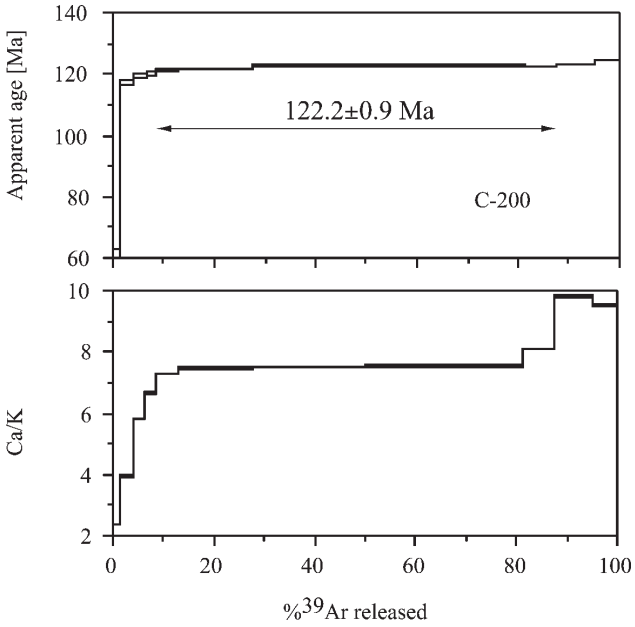

Fig. 6. $^{40}Ar/^{39}Ar$ results for sample C-200. (**a**) Age spectrum. (**b**) Ca/K vs. % ^{39}Ar released.

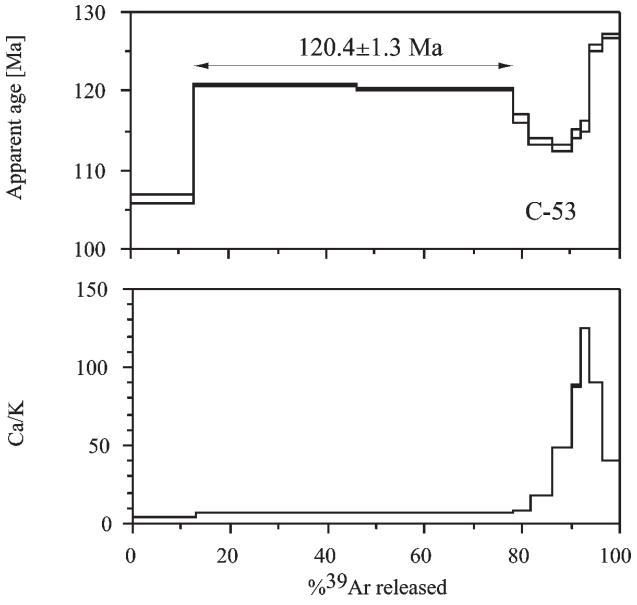

Fig. 7. $^{40}Ar/^{39}Ar$ results for sample C-53. (**a**) Age spectrum. (**b**) Ca/K vs. % ^{39}Ar released.

The most stable part of the age spectrum consists of two steps, which contain most of the ^{39}Ar released (65 % ^{39}Ar released). Their Ca/K ratios are 6.1 and 6.2 (Table 2), which is in a good agreement with the ratios obtained by electron microprobe (Table 1). 120.4±1.3 Ma age was obtained for these two steps.

Interpretation

All four ages obtained for two lithological types of the TAR are indistinguishable within error limits (Fig. 8). Because dated samples represent small sub-volcanic intrusions, which must have undergone rapid cooling, we interpret the 120–122 Ma age (upper Barremian/lower Aptian) as reflecting time of magmatic emplacement of TAR. However, field relationships indicate that the syenite could be younger (syenite forms small dyke intruding mesocratic teschenite). Taken at face value, the age obtained for more evolved magma (syenite) is 1.9±2.1 Ma younger than the average of three mesocratic teschenite. We were unable to date the intruded teschenite from the same outcrop due to very advanced alterations. Nevertheless, our dating results strongly suggest that the evolution of the alkaline magma from mesocratic phase (represented by teschenites) to leucocratic phase (represented by syenite) was fast and happened within few Ma.

Conclusions

Alkaline lamprophyres in the Silesian Nappe of the Polish Western Carpathians are represented dominantly by mesocratic teschenites and rarer by leucocratic syenites. $^{40}Ar/^{39}Ar$ stepwise heating dating of three teschenite samples resulted in indistinguishable ages of 122.0±1.5, 122.4±1.1, 122.2±0.9 Ma.

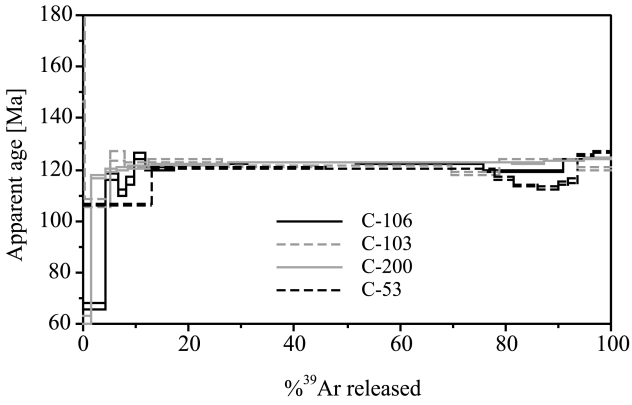

Fig. 8. $^{40}Ar/^{39}Ar$ age spectra for all samples.

The syenite sample yielded statistically indistinguishable age of 120.4±1.3 Ma. Thus, time period between ca. 120 and 122 Ma is interpreted as the time of magmatic emplacement of TAR. This suggests rather fast parent magma evolution from meso to leucocratic stage.

Although we did not date the most primitive, picritic, rocks representing melanocratic type of TAR province (exposed in the Czech Republic), it seems to be reasonable to assume, that the rate of magma evolution from melanocratic to mesocratic stage, was not significantly different from the rate, at which these rocks evolved from meso- to leucocratic phase. Hence it is likely that the TAR were emplaced within a very short time period, possibly less than 5 Ma during the Early Cretaceous extensional episode within the Silesian Basin.

Acknowledgments: This research was funded by KBN Grant No. 6PO4D 014 12. Reviews by H. Maluski, A. Mulch and J. Spišiak helped to improve the manuscript.

References

Belluso E., Ruffini R., Schaller M. & Villa I.M. 2000: Electron-microscope and Ar isotope characterization of chemically heterogeneous amphiboles from the Palala shear zone, Limpopo Belt, South Africa. *Eur. J. Mineral.* 12, 1, 45–62.

Burtanówna J., Konior K. & Książkiewicz M. 1937: Geological map of the Silesian Carpathians. *Silesian PAU,* Kraków (in Polish).

Csontos L., Nagymarosy A., Horvath F. & Kováč M. 1992: Tertiary evolution of the intra-Carpathian area: a model. *Tectonophysics* 208, 221–241.

Dostal J. & Owen J.V. 1998: Cretaceous alkaline lamprophyres from northeastern Czech Republic: geochemistry and petrogenesis. *Geol. Rdsch.* 87, 67–77.

Hohenegger L. 1861: Die geognostischen Verhaltnisse der Nordkarpaten in Schlesien und den angrenzenden Teilen von Mahren und Galizien als Elauterung zu der geognostischen Karte der Nordkarpaten. *J. Perthes. Gotha.*

Hovorka D. & Spišiak J. 1988: Volcanism of Mesozoic of the Western Carpathians. *VEDA,* Bratislava, 1–263.

Kudělásková J. 1987: Petrology and geochemistry of selected rock types teschenite association, Outer Western Carpathians. *Geol. Zbor. Geol. Carpath.* 38, 5, 545–573.

Mahmood A. 1973: Petrology of the Teschenitic rock series from the type area of Cieszyn (Teschen) in the Polish Carpathians. *Ann. Soc. Geol. Pol.* 43, 2.

Książkiewicz M. 1972: Geology of Poland. Vol. IV. Tectonics, Part 3: Carpathians. *Wydawnictwa Geologiczne,* Warszawa, 1–228 (in Polish).

Leake B E., Woolley A.R., Arps C. E.S., Birch W.D., Gilbert M.C., Grice J.D., Hawthorne F.C., Kato A., Kisch H.J., Krivovichev V.G., Linthout K., Laird Jo., Mandarino J.A., Maresch W.V., Nickel E.H., Rock N.M.S., Schumacher J.C., Smith D.C., Stephenson N.C.N., Ungaretti L., Whittaker E.J.W. & Youzhi G. 1997: Nomenclature of amphiboles: Report of the Subcommittee on Amphiboles of the International Mineralogical Association, Commission on New Minerals and Mineral Names. *American Mineralogist* 82, 1019–1037.

Nowak W. 1978: Teschenites in the Polish Western Carpathians, occurrence and problem of stratigraphic position. In: Nowak W.A. & Wieser T. (Eds.): Conference materials. *Kraków 22–24. 04. 1978,* (in Polish).

Smulikowski K. 1980: Remarks on Teschen magmatic province (in Polish). *Ann. Soc. Geol. Pol.* L-1, 41–54.

Suk M. 1984: Geological history of the territory of the Czech Socialist Republic. *Geological Survey,* Prague, 1–396.

Šmíd B. 1962: Geology and petrography of the Teschenite Association Rocks at the northern foot of Beskydy. *Geol. Práce, Zoš.* 63, 53–60 (in Slovak).

Tschermak G. 1866: Felsarten von ungewohnlicher Zusammensetzung in der Umgebung von Teschen und Neutitsche. *Sitz-Berg K Akad Wiss Math-Naturwiss Kl* 53, 1, 1-5, 260–287 (in German).

Villa I.M., Hermann J., Müntener O. & Trommsdorff V. 2000: ^{39}Ar-^{40}Ar dating of multiply zoned amphibole generations (Malenco, Italian Alps). *Contr. Mineral. Petrology* 140, 363–381.

Wieser T. 1971: Alterations of teschenites in the Polysch Carpathian Flysch (in Polish). *Kwart. Geol.* 15, 901–921.

Żytko K., Zając R., Gucik S. 1989: Map of the tectonic elements of the Western Outer Carpathians and their foreland, 1:500,000. *Państwowy Instytut Geologiczny*, Warszawa.